Characteristics of the 64 pixel PIN Diode

Pascal Renschler

November 8, 2007

This paper briefly summarizes the main results of [2] concerning the Segmented PIN Diode (SPD) used at the pre-spectrometer test setup for the KATRIN experiment [1]. It is focusing on the presentation of the results on the detector performance and excludes detailed descriptions of the technical setups. Furthermore, DAQ related work and results of the MCP are not considered.

1 Detector status and UHV suitability

The SPD was successfully installed and cooled in the detector chamber. The temperature reached with a detector ready for data taking was 217 K which is close to the targeted temperature of 213 K. Typical waiting times after setting new setpoints for the detector temperature are around 200 minutes. The liquid Nitrogen circuit works and needs to be refilled every 13-18 h depending on the detector heat load and if the used lN_2 is returned to the dewar.

Two safety circuits were installed shutting off the power supplies if either the detector temperature rises above 283 K or the power drain of the preamplifiers exceeds 3A. This allows safe longtime operation of the SPD system without human observation.

To test the UHV suitability two Residual Gas Analysis (RGA) were taken at 217 K and 303 K with a slightly heated detector ceramic. The chamber including the detector was not baked out before in order to prevent an unlikely but possible contamination of the detector chamber with substances coming from the SPD electronics. The RGA showed no anomalies above 50 u, so the analysis concentrates on the masses ranging from 1-50 u. The first RGA was taken at 217 K at a pressure of $p_{cold} = 6 \times 10^{-10}$ mbar (see fig. 1(a)). The system had an air leak at that time and the resulting RGA is well in the normal bounds. With a heated detector at 303 K, which corresponds to a pressure of $p_{hot} = 8.3 \times 10^{-8}$ mbar, the O_2 peak at 32 u rises above average. The normal $N_2 : O_2$ ratio of a system with an air leak should be 5 : 1. This points toward an additional source of O_2, arising from the detector ceramics since this is the only heated part. The rest of the detector chamber was at room temperature.

The SPD is suitable for the pre-spectrometer test experiment regarding vacuum conditions. To reduce the gas load on the spectrometers, the valve between detector chamber and the prespectrometer should only be opened while having a cooled detector. However, further measurements of the UHV characteristics of ceramics, solders, flux material and SMD components in a purpose-built vacuum oven combined with improved vacuum handling and cleaning procedures while and after the SPD assembly should improve the UHV suitability. This is for example necessary to use the SPD system for the commissioing of the main spectrometer.

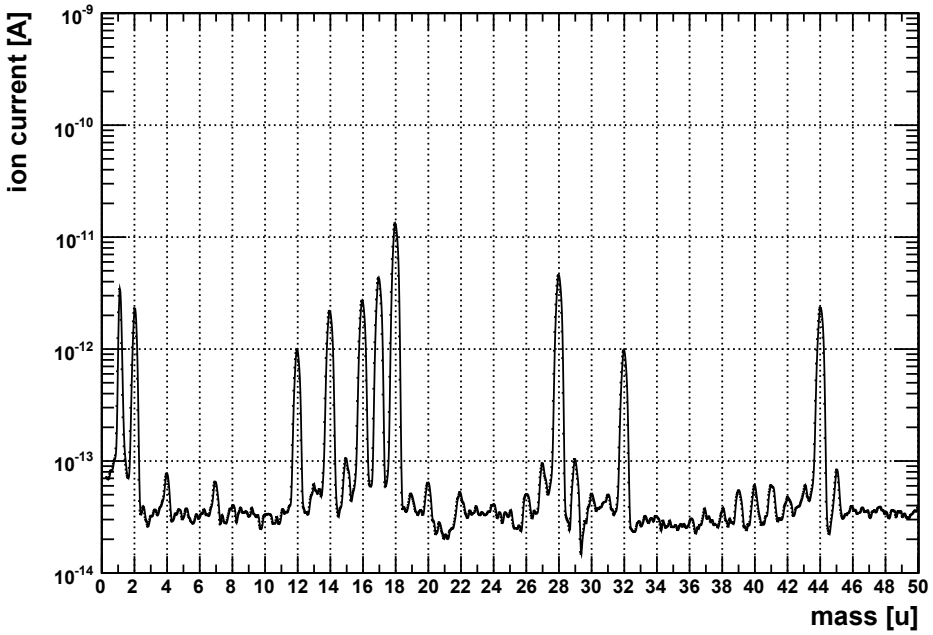

(a)

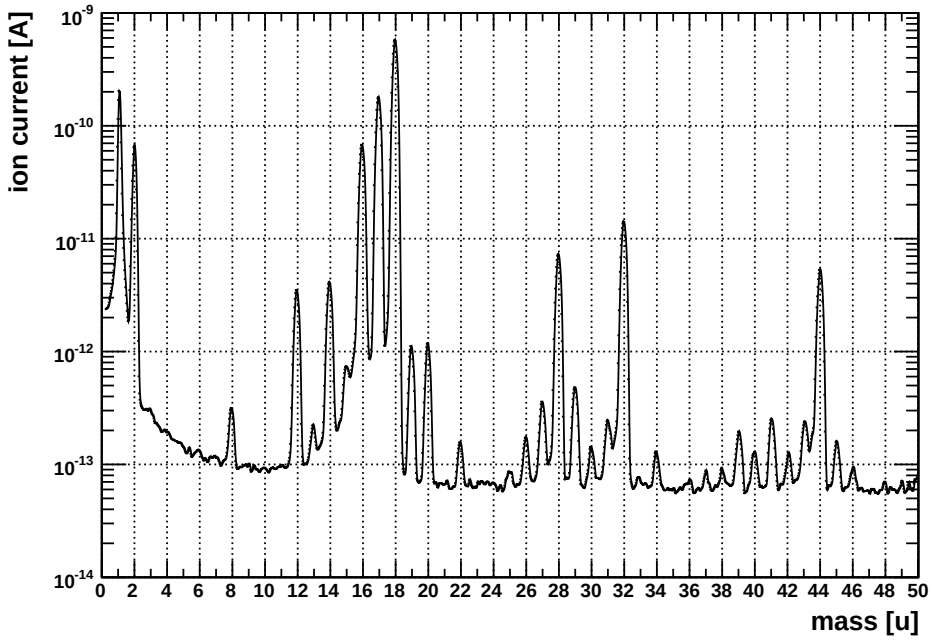

(b)

Figure 1: Two RGA of the detector chamber with installed SPD at (a) a detector temperature of 217 K and a pressure of 6×10^{-10} mbar and (b) at 303 K and $8,3 \times 10^{-8}$ mbar.

2 Energy calibration and energy resolution

For the following measurements, the detector chamber was used in stand-alone mode, i.e. it was not attached to the pre-spectrometer. Thus it was possible to place an ^{241}Am calibration source with different exit windows (see tab. 1) in front of the SPD for calibration and characterization purposes. A Be-window acts as separation to ambient side. Depending on the chosen exit window material the rate of x-rays onto the detector is in the range between 2-9 Hz per pixel. A superimposed plot showing the ADC spectra of all used exit windows of the Am-source is given in fig. 2.

The spectra of five exit windows were measured with all 64 pixels at 217 K detector temperature. Due to fitting gauss functions to the peaks of every window and pixel, there is an energy calibration available for all data taken with the SPD. The difference of the reconstructed energy after the energy calibration from the calibration lines is below $\pm 0.5\%$. An energy calibration using only 2 exit windows instead of 5 shows a deviation in the same regime, so both methods are suitable.

The according relative energy resolution $\Delta E/E$ at FWHM for all 64 pixel is shown in fig. 3. Tab. 1 shows the absolute energy resolution ΔE. The average absolute energy resolution of the 64 pixels is $\Delta E \approx 4.4\,\text{keV}$, but the pixels 37 (E5), 45 (F5) and 47 (F7) show an increased energy resolution of about 6-7 keV. These pixels also can't resolve the Rubidium peak because it is overlapped by electronic noise.

3 Temperature and bias voltage dependence of the energy resolution

To find possible sources for the moderate energy resolution it was measured in dependence to the detector temperature. The measurement shows, that the energy resolution is not dependent on the detector temperature (see fig. 4). This indicates that the leakage current is dominated by other than thermal effects.

For bias voltage the manufacturer recommends 20 V. The SPD already reaches full depletion at 10 V. While increasing the bias voltage in the measurement, one pixel was dominated by noise at 14 V. At 16 V 20 pixels had to be excluded from the measurement. A higher bias voltage setting was not reachable. Fig. 5 shows the energy resolution for the 44 pixels that performed well up to 16 V. Again, there is no noticeable improvement in the energy resolution. The reason for the bad performance at higher bias voltages is unclear. One explanation which the manufacturer supports are mechanical tensions inside the wafer that have occurred during the gluing of the wafer upon the ceramic.

Table 1:

Element	E_R **[keV]**	**gew. gem. aus**	ΔE **[keV]**	$\Delta E/E_R$ **[%]**
^{37}Rb	$13,585$	$K_{\alpha_{1,2}}$,$K_{\beta_{1,2,3}}$	$4,10 \pm 0,32$	$30,2 \pm 2,4$
^{42}Mo	$17,765$	$K_{\alpha_{1,2}}$,$K_{\beta_{1,2,3}}$	$4,23 \pm 0,31$	$23,8 \pm 1,8$
^{47}Ag	$22,565$	$K_{\alpha_{1,2}}$,$K_{\beta_{1,2,3}}$	$4,46 \pm 0,35$	$19,8 \pm 1,6$
^{56}Ba	$32,061$	$K_{\alpha_{1,2}}$	$4,81 \pm 0,57$	$15,0 \pm 1,8$
^{65}Tb	$44,216$	$K_{\alpha_{1,2}}$	$4,33 \pm 0,31$	$9,8 \pm 1,7$

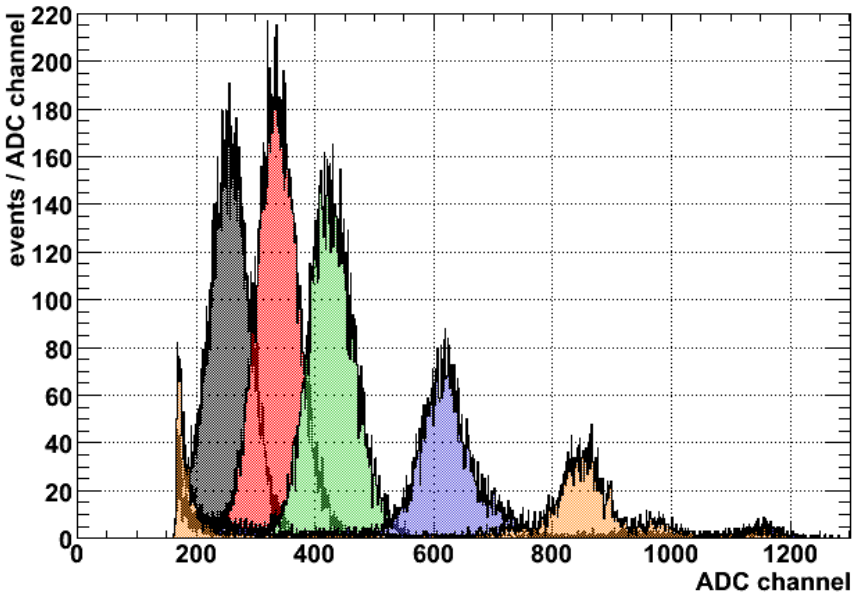

Figure 2: Superimposed ADC histograms of the x-ray energies representing the different exit windows. ^{37}Rb(black), ^{42}Mo (red), ^{47}Ag (green), ^{56}Ba (blue) und ^{65}Tb (orange).

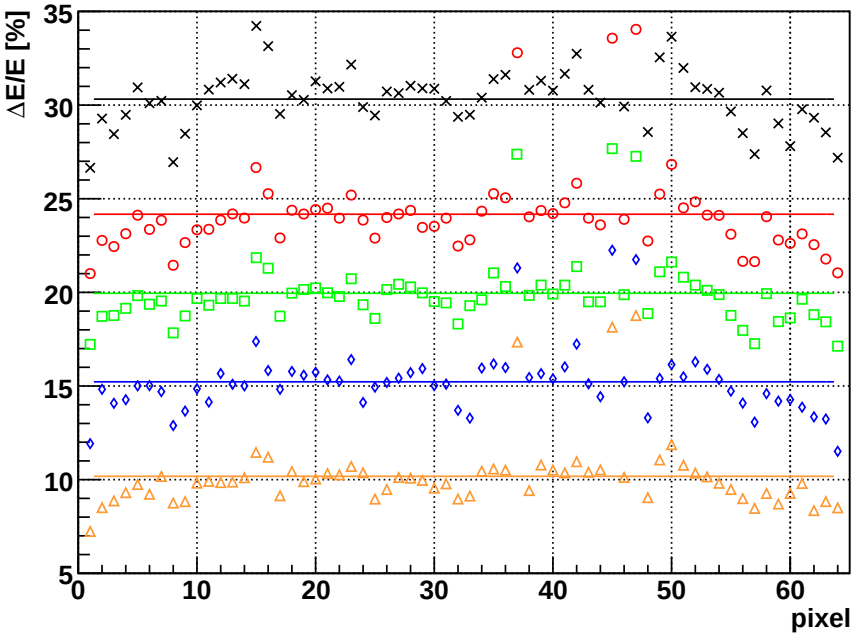

Figure 3: Relative energy resolution of the 64 SPD pixels for five energies. ^{37}Rb (black), ^{42}Mo (red), ^{47}Ag (green), ^{56}Ba (blue) and ^{65}Tb (orange)

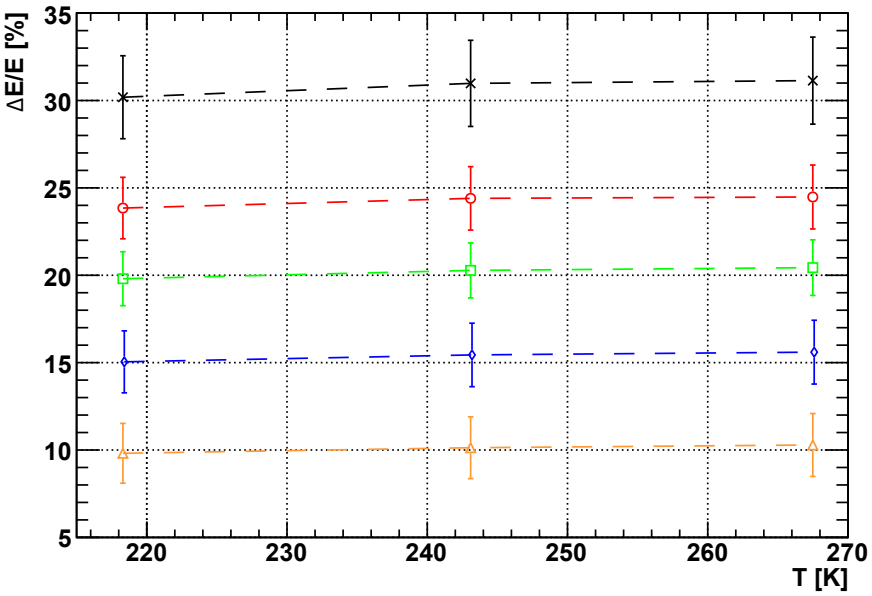

Figure 4: Relative energy resolution for different detector temperatures and energies. ^{37}Rb (black), ^{42}Mo (red), ^{47}Ag (green), ^{56}Ba (blue) and ^{65}Tb (orange). The dotted lines guide the eye.

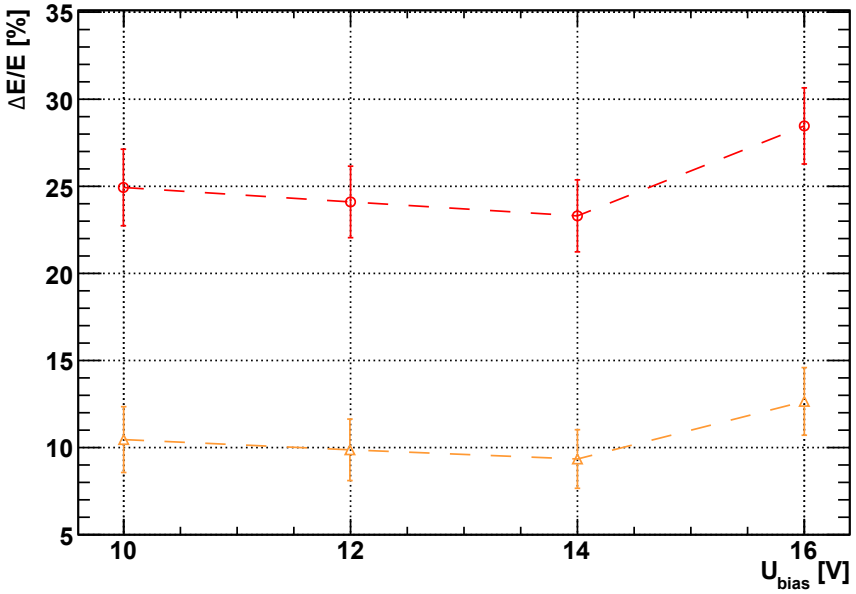

Figure 5: Relative energy resolution for different bias voltages. ^{42}Mo (red) and ^{65}Tb (orange). The dotted lines guide the eye.

4 Background

Fig. 6 shows pixelnumber in which two consecutive events happened relative to the first event (marked as 0). The clear peaks at surrounding pixels indicate a kind of cross-talk or induction between the pixels. All pixels show the same behaviour, so not a few pixels are responsible for the distribution. This will be investigated further in the pre-spectrometer setup.

A 16,5$\dot{\text{h}}$ background measurement is shown in fig. 7(a) for a typical pixel. The important energy intervall from 15-22 keV shows an increased event rate. The scatterplot with energy over time (fig. 9) shows a timely structure corresponding to noise bursts up to 70 keV. A burst consists of about 20 events with an almost linear decrease in energy (fig. 8(a)).

The origin of the burst are subject of investigations, as they had not been observed when the detector was replaced by capacitors.
For background analysis these bursts can be clearly identified and removed by a noise cut that excludes all events that have a time difference smaller than 0.3 s from each other and are happening in the same pixel. The SPD (without the 3 mentioned pixels with worse performance) has an eventrate in the energy intervall from 15-22 keV of

- $(439.8 \pm 2.7) \times 10^{-3}$ events/s over all pixels and
- an average of $(7.21 \pm 0.05) \times 10^{-3}$ events/s per pixel.

After applying the noise cut, this reduces to

- $(20.3 \pm 0.6) \times 10^{-3}$ events/s over all pixels and
- an average of $(0.33 \pm 0.01) \times 10^{-3}$ events/s per pixel.

The loss of background data when applying this cut is about 0.22%. When using higher rates (e.g. from the e-gun), the data loss is too high and the noise has to be treated as background. At a 1 kHz e-gun rate, this corresponds to a $10^6 : 1$ signal-to-noise ratio.

A comparison of the whole pixel array with adapted results of simulations in [3] are displayed in fig. 10. The simulation assumed a 100 mm lead shielding around the detector. The simulation is still comparable to the actual setup, because it discovered that 80% of the background is coming from the ceramic itself. The measurement is in agreement with the simulation and shows the challenge to reduce the intrinsic background rate for the Focal Plane Detector (FPD) to 1 mHz.

References

[1] KATRIN Collaboration. KATRIN Design Report 2004. Technical Report FZKA 7090, Forschungszentrum Karlsruhe, 2005.

[2] P. Renschler. Inbetriebnahme und Charakterisierung von Detektorsystemen für elektromagnetische Tests von Spektrometern. Diploma Thesis, Universitaet Karlsruhe, 2007.

[3] F. Schwamm. *Untergrunduntersuchungen für das KATRIN-Experiment.* Dissertation, Forschungszentrum Karlsruhe, 2004.

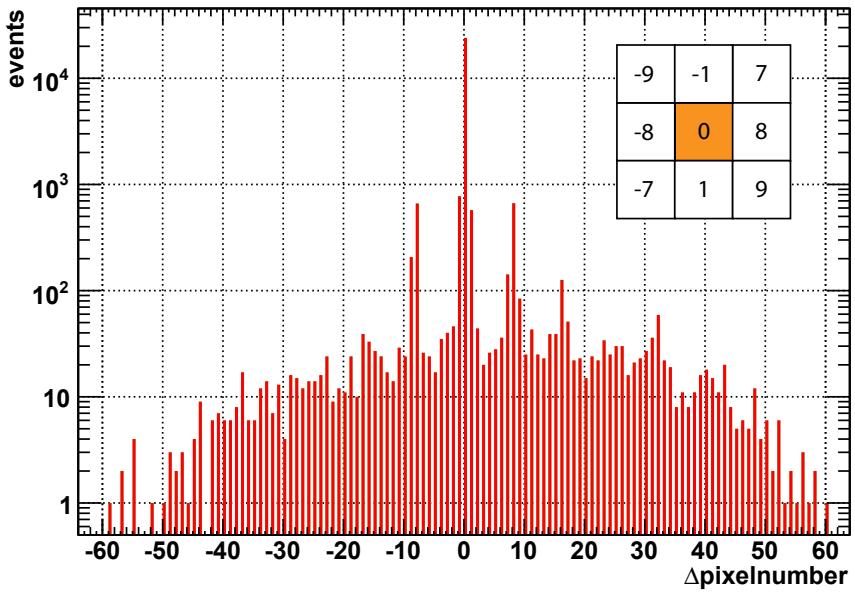

Figure 6: Subtracted pixelnumbers of consecutive events in the 15-22 keV energy intervall. The upper right corner shows the relative pixelnumbers that are not on the edge of the wafer. Zero corresponds to consecutive events in the same pixel.

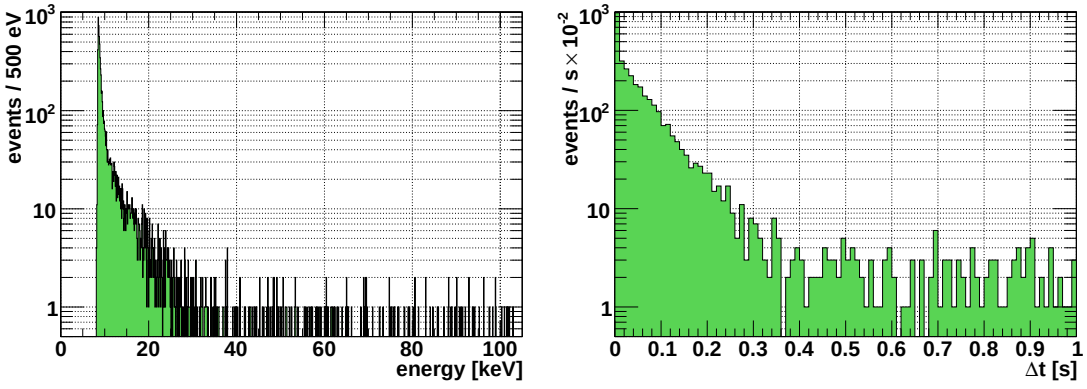

(a) (b)

Figure 7: (a) Background spectrum and (b) time difference of to conescutive events of pixel D5.

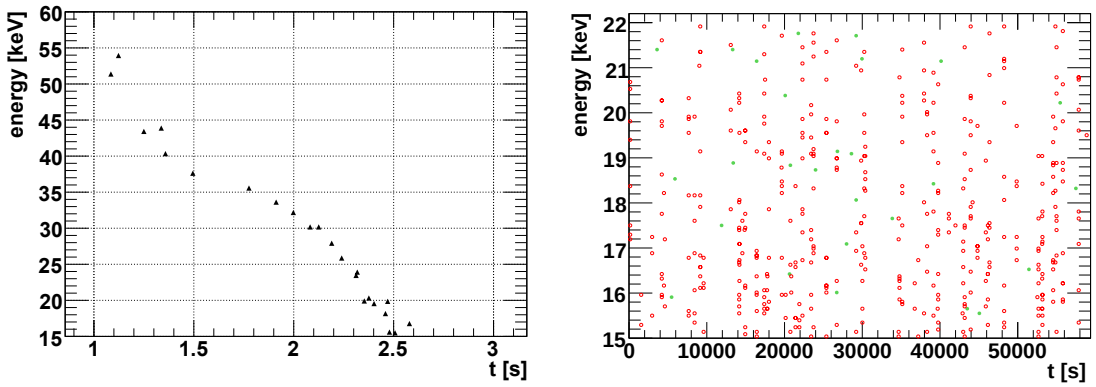

(a) (b)

Figure 8: (a) Typical noiseburst showing a linear decrease in energy over a 2 s time interval. (b) Accepted and rejected events by the noise cut in the 15-22 keV energy interval. 410 events were rejected (red) and 27 (green).

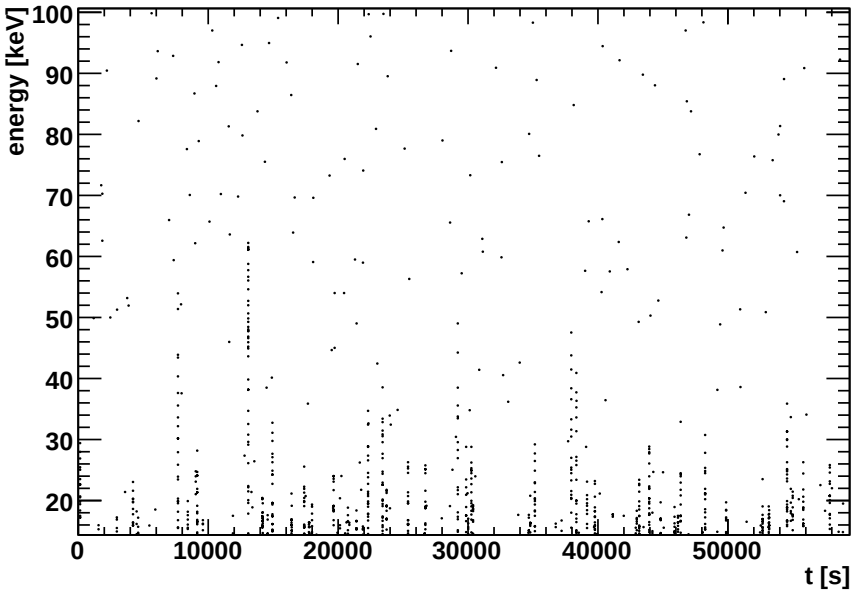

Figure 9: Scatterplot of energy over time for pixel D5. The vertical structure indicates timely correlations.

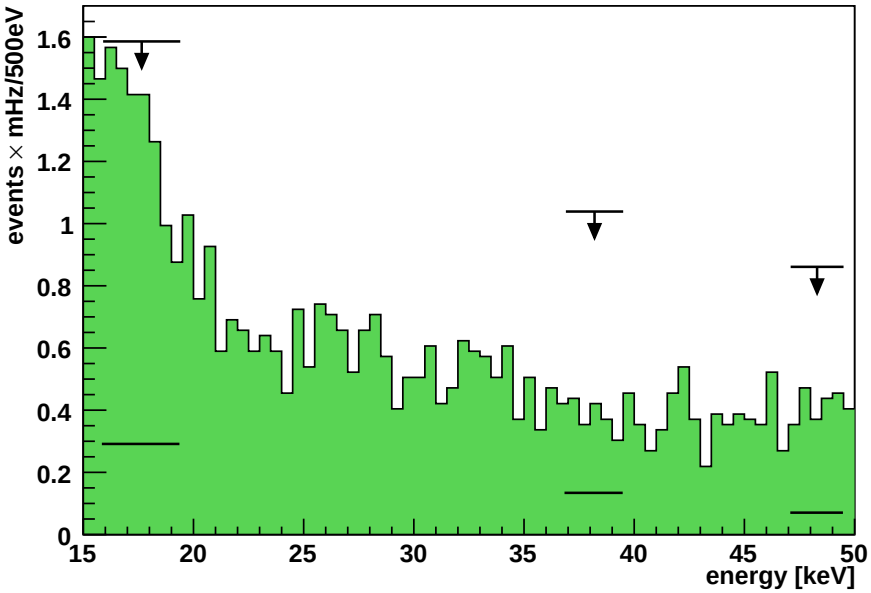

Figure 10: Comparison of the measured background rates of the SPD with simulations [3]. The experimental data is shown in green. The simulated upper level corresponds to the maximum expected activity (99% C.L.) and the expected values correspond to an average activity of ^{238}U and ^{232}Th.